Available online at www.sciencedirect.com

ScienceDirect

Procedia CIRP 24 (2014) 49 – 55

www.elsevier.com/locate/procedia

New Production Technologies in Aerospace Industry - 5th Machining Innovations Conference (MIC 2014)

Drilling of Inconel 718 with geometry-modified twist drills

Nicolas Beer[a,]*, Ekrem Özkaya[a], Dirk Biermann[a]

[a]*Institute of Machining Technology, Dortmund 44227, Germany*

* Nicolas Beer, phone: +49-231-755-5518; fax: +49-231-755-5141; *E-mail address:* beer@isf.de

Abstract

The drilling process of Inconel 718, a nickel-based superalloy, is very challenging due to the material properties, the operating conditions and the high quality requirements. Carbides within the material matrix cause an excessive amount of abrasive tool wear. Moreover, a large amount of the heat caused by the machining process, especially in drilling, has to be dissipated by the tool and the coolant, due to the low thermal conductivity of Inconel 718. This high thermal load also restricts the cutting speed. The combination of all attributes limits productivity and economic efficiency when drilling Inconel 718 with cemented carbide twist drills.

This paper presents a method to adapt twist drills considering the mentioned demands by using geometry-modified tools. The aim is to increase the resistance against abrasive wear and to reduce the thermal loads; so that, tool life and bore quality can be improved. The analysis of the new tool geometry was realized by advanced Computational-Fluid-Dynamics (CFD) simulations. The simulations provide detailed information about the coolant flow and consequently the improved cooling of tool regions which are, on the suggested geometry, exposed to very high thermal loads. Experiments showed that the tool life can be increased by up to 50% in contradiction to a standard twist drill. The improvement on the bore quality was shown by determining the roundness deviation and the average surface roughness. In addition, micro hardness tests and metallurgy preparations were conducted to investigate the surface integrity of the bore surface layer. Although the presented geometry only represents a prototype status, the results are impressive. The tool life and the bore quality have been improved, and the simulations showed clearly that there is a significantly better coolant flow, when using the new geometry.

Selection and peer-review under responsibility of the International Scientific Committee of the "New Production Technologies in Aerospace Industry" conference in the person of the Conference Chairs: Prof. Berend Denkena, Prof. Yusuf Altintas, Prof. Pedro J. Arrazola, Prof. Tojiro Aoyama and Prof. Dragos Axinte

Keywords: nickel-based alloy; drilling; twist drill; cemented carbide; cooling; surface integrity; Computational-Fluid-Dynamics; turbulence models

1. Introduction

The machining of difficult-to-cut materials such as the superalloy Inconel 718 is very challenging because of the characteristics of the workpiece material and the high quality demands for the process results. Especially when drilling with cemented carbide drills productivity and tool life are very limited. Within this paper a method to modify twist drills with respect to a new flank face geometry is presented. Here the flank wear is controlled and limited to a defined maximum. Additionally, with the modified geometry, the critical areas of the tool are provided with a larger amount of coolant without increasing the total volume of coolant needed [1, 2, 3, 4].

Inconel 718 was developed for applications in aerospace turbines; and later, it has been used in a wide range of applications due to its outstanding material properties. Examples beside the aerospace and gas turbine industry are automotive applications, and the medical and chemical industries. The mechanical properties such as creep-, tensile-, fatigue- and rupture-strength remain on a high level for temperatures up to 700 °C [1]. During machining, different material characteristics of Inconel 718 lead to very high thermo-mechanical tool loads and a high wear rate, e.g. work hardening and the high-

Selection and peer-review under responsibility of the International Scientific Committee of the "New Production Technologies in Aerospace Industry" conference in the person of the Conference Chairs: Prof. Berend Denkena, Prof. Yusuf Altintas, Prof. Pedro J. Arrazola, Prof. Tojiro Aoyama and Prof. Dragos Axinte
doi:10.1016/j.procir.2014.07.124

temperature strength. Additionally, a large amount of heat has to be dissipated by the tool and the coolant because of the low thermal conductivity of the workpiece material. Abrasive and adhesive mechanisms dominate the wear as a result of the high amount of carbides within the metal matrix and the adhesive tendency of the large portion of nickel in the alloy [3, 4, 5, 6]. Especially when drilling Inconel 718 high tool loads lead to low productivity and limited tool life. Due to the high temperatures in the cutting zone, the cutting speed has to be limited up to $v_c = 50$ m/min. Typically used feed rates are around $f = 0.10$ mm/rev [2, 7]. In order to reduce the thermal load and support the chip evacuation an internal cooling with high pressure is commonly applied. The use of MQL or no coolant leads to a large amount of subsurface damage and very short tool life [7, 8].

When drilling with twist drills, internal cooling channels are used to supply sufficient cutting fluid to the cutting zone. The exits of these channels are located on the flank face which leads to an indirect cooling of the cutting zone. To enhance the cooling effect and to reduce the thermal load different design elements can be used. By changing the geometry, the diameter and the location of the cooling channels a higher coolant flow rate and convection can be achieved. Furthermore, the form of the flutes, the end and length of the cooling channels and even the form of the tool chuck influence the efficiency of the cooling [9, 10, 11]. A major drawback when supplying the coolant via the flank face of a tool is the poor cooling effect. Because of the small gap between tool and workpiece the velocity of the coolant has to be twice as large as the maximum cutting speed to fill this gap properly. *Obikawa* and *Yamaguchi* proved this fact by a CFD-simulation of a turning process [12]. The method presented here shows a way to improve the wear resistance of cemented carbide drills and to improve the efficiency of the supplied coolant fluid. This is achieved by a new flank face geometry. The influence on the tool wear, the bore roundness deviation and average surface roughness and the surface integrity will be presented, as well. Additionally a CFD-simulation was used to analyze the influence on the coolant flow in detail.

2. Experimental procedure

2.1. Workpiece material

The workpiece, a round plate consisting of Inconel 718, had a diameter of $d = 200$ mm and a thickness of $t = 34$ mm. The fully annealed material fulfils the standards of the aerospace industry with respect to the metallurgic composition, heat treatment and mechanical properties. Some selected properties are listed in Table 1.

Table 1. Selected properties of the workpiece material Inconel 718

Property	Value
Ultimate tensile strength at room temperature	$R_{m,RT} > 1400$ N/mm²
Ultimate tensile strength at T = 649 °C	$R_{m,649°C} > 1100$ N/mm²
Elongation	a = 17…23 %
Hardness	H > 450 HV30
Thermal conductivity	$\lambda = 11.1$ W/(m · K)
Thermal expansion	$\alpha = 12.6 \cdot 10^{-6}$ K^{-1}

2.2. Twist drill design

The improvement of cemented carbide twist drills by a modification of the flank face was tested on drills with a diameter of $d = 6.8$ mm for a maximum drilling depth of $l = 34$ mm ($l/D = 5$) provided by Guehring KG, Albstadt, Germany. Macro- and micro-geometry of the tools comply with a standard tool designed for the machining of difficult-to-cut materials. The used cemented carbide had an amount of 5 % Cobalt and an average grain size of $d_m = 0.5$ µm. For an elimination of potential influencing factors, no coating has been applied. Furthermore the flutes were ground to achieve a median surface roughness below $Rz = 0.5$ µm. The low surface roughness has been chosen to improve the chip evacuation and to reduce the risk of chip jamming and a resulting tool failure.

The modified flank faces are inspired by a similar modification on cutting inserts for turning and milling. The utilization of a flank face backspace in a defined distance to the cutting edge this modification limits the maximum width of flank face wear. Due to this, process forces and the impact on the subsurface integrity can be hold on a constant level and tool life can be extended. Improvements in tool life range between 40 % and 250 % depending on the process and the workpiece material [13, 14, 15, 16].

To adapt such a flank face geometry for a twist drill, several specific features when drilling have to be considered. Due to the changing cutting speed and the varying geometry the mechanical load differ along the cutting edge [17, 18]. Especially when drilling Inconel 718 the process forces are very high. Previous experiments showed feed forces up to 2500 N when a worn tool was used. Furthermore the tool wear in drilling differs in many ways from that in turning or in milling processes [6, 7, 19, 20, 21]. The resulting flank face modification based on all the above mentioned factors is shown in Fig. 1.

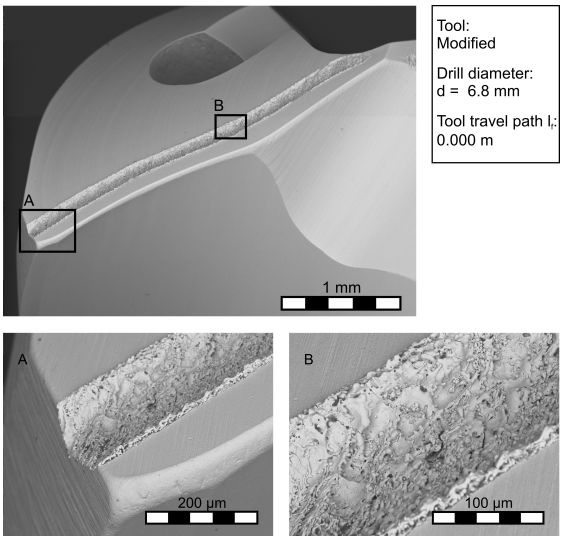

Fig. 1. Twist drill with modified flank face

As can be seen within the overview picture (Fig 1. upper

part) a groove has been implemented on the flank face parallel to the cutting edge at a distance of l = 150…200 µm. The secondary cutting edge has a negative chamfer and thus reduces the distance of the groove to 100 µm in the vicinity of the outer corner, see detail **A**. The groove has been manufactured by laser melting which results in a rough surface and small burrs as can be seen in detail **B**. The depth of the groove is about d = 50 µm. Because of the clearance angle a relocation of the whole flank face is not necessary.

2.3. Experimental setup

The experiments were realized on a machining centre, type BZ40CS, manufactured by Grob, Mindelheim, Germany. Cutting parameters were chosen to v_c = 35 m/min and f = 0.10 mm/rev with an internal cooling supply of p = 40 bar. The water-based emulsion used had a concentration of 5 %. The manufactured through-bores had a total depth of l = 34 mm. The abort criteria for tool wear measurement were chippings along the cutting edge, especially close to the outer corner, or a maximum width of flank wear land of VB_{max} = 300 µm. Because of the limited width of flank wear land when using the modified tools, the abort criterion for them was the first appearance of flank wear behind the groove. However, this fulfils the criterion of VB_{max} = 300 µm, too.

3. CFD-Simulation

In the field of production engineering, the CFD-analysis is a relatively new and effective tool to investigate the heat flux and the coolant flow in manufacturing systems and processes [22, 23]. *Özkaya et al.* have already shown in their studies that CFD can be utilized to optimize tools for machining process [24, 25, 26, 27]. Within this study the CFD is used to analyze and visualize the complex coolant flow of two different twist drills. In order to obtain accurate and reliable results, the numerical computations should be performed on a high quality mesh, which is also very challenging with respect to the complex geometry of the drilling tools [28, 29]. Another very important point is the choice of an appropriate turbulence-model [23, 30].

3.1. Geometry model, boundary conditions and meshing

Both drills (see Fig. 2) are computationally modeled for a length of l = 20 mm. The computational models provided by Guehring were imported into the ANSYS/CFX simulation environment. A negative model, the so called fluid geometry (light blue) was created out of the solid body model (grey), shown in Fig. 2 (**P1**), by using a cavity fill. The essential boundary conditions are prescribed (**P2**). To achieve an ideal alignment and to resolve the flow completely, the mesh was sufficiently refined in area **A** (**P3**), where high turbulence zones and gradients exist. Patch independent tetrahedron elements in combination with the inflation layer method, which is suited for fine calculations in near-wall regions, were used for the discretization. On contrary, there are only small variations of fluid variables existing in the domain **B** (**P3**). For the areas of the computational domain, where steep gradients do not occur, a relatively coarse mesh is sufficient. Therefore, away from wall-boundary layers, the domain was meshed with a sweep method so that a reasonably fine mesh which led to sufficiently accurate numerical results within affordable computational cost was obtained. Following, the above discussion on the spatial discretization, employed mathematical models and the solver parameters, especially turbulence models, are introduced in the next sections (Fig.2).

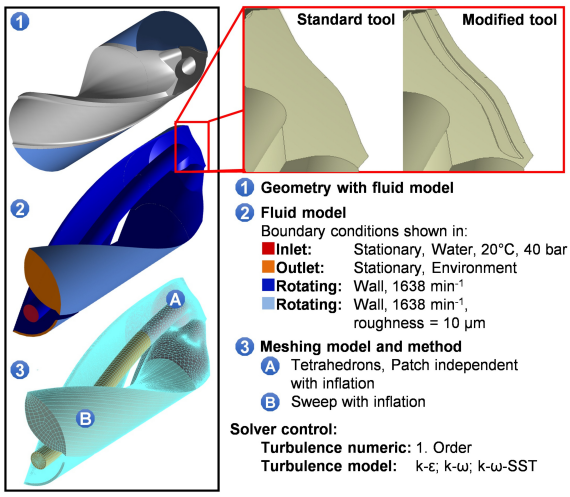

Fig. 2. Boundary conditions and meshing zone

3.2. Turbulence model

The Reynolds Averaged Navier Stokes (RANS) models are very often employed to mathematically described, industrial flow problems in the turbulent regime [23]. The RANS equations must be closed with an additional transport equation for the turbulent quantities. For this purpose the turbulence models k-ε-, k-ω- or k-ω-shear-stress-transport (SST) are usually used, where the turbulent kinetic energy is described by k and the isotropic dissipation is described by either ε or ω [23, 31]. The k-ε model is more accurate for resolving the flow away from the boundary layer. In addition to the transport equation for the turbulent energy, the energy-dissipating vortex is resolved using the characteristic frequency. For calculations in near-wall areas (fringes), which are accurately meshed, the k-ω model is suited best [32]. The k-ω-SST turbulence model provides an opportunity to combine the two preceding models; it considers the near-wall areas and areas being away from the wall. It is, therefore, an ideal candidate for numerical simulations in our scope.

3.3. Numerical model of turbulence intensity

The flow can be specified by different parameters as the Reynolds number Re, the kinetic energy k and the turbulence intensity I; so that, a direct comparison of different turbulence models is possible. The equation of turbulence intensity I (5) contains the irregular variations of the vortexes and is calculated using the ratio between turbulent strength u_{rms} (3) and mean velocity $\bar{u}$ (1). The turbulent strength is defined as the

root mean square (rms) of the temporal turbulent fluctuation $u'(t)$ (2). The Reynolds number Re (4) is the ratio of mean velocity $\bar{u}$ multiplied with the characteristic length D_H and the kinematic viscosity v. The kinetic energy k (6) is the square value of the product of the maximum velocity v_{max} and the turbulence intensity I, which is then multiplied with a factor of 1.5. The volumetric flux Q is given through the double integral (7). The velocity is a continuous variable for which the mean value is supposed to be calculated according to the *mean value theorem*. Our numerical results are obtained on a computational grid which provides only point-wise values; thus, the right hand side of (1) has been employed.

Continuous record	Discrete points	
$\bar{u} = \frac{1}{T}\int_t^{t+T} u(t)\,dt$	$= \frac{1}{N}\sum_1^N u_i$	(1)
$\lvert u'(t)\rvert = u(t) - \bar{u}$	$\lvert u'_i\rvert = u_i - \bar{u}$	(2)
$u_{rms} = \sqrt{\overline{u'(t)^2}}$	$= \sqrt{\frac{1}{N}\sum_{i=1}^N (u'_i)^2}$	(3)

$$Re = \frac{\bar{u} D_H}{vA} \quad (4)$$

$$I = \frac{u_{rms}}{\bar{u}} \quad (5)$$

$$k = \frac{3}{2}(v_{max}\, I)^2 \quad (6)$$

$$Q = \iint_A \bar{u}\, d\vec{A} \quad (7)$$

4. Experimental results

4.1. Tool wear

The tool wear was tested by the application of four drills. Two standard tools are compared against two modified ones. The maximum width of flank wear land over the drill path was measured regularly at a distance of l_f = 0,170 m. The results are shown in **Fig. 3.**

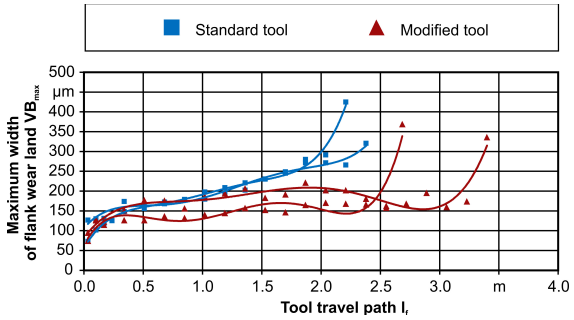

Fig. 3. Flank wear over tool travel path

As it can be seen the standard tools show very similar progression of wear and reach tool life travel paths between L_f = 2.210…2.380 m before the abort criterion in tool wear of VB_{max} = 300 µm was exceeded. When using the modified tools the wear differs significantly in comparison to the standard tools. Both drills show a relatively constant maximum width of flank wear land over the tool travel path. This is caused by the limitation due to the groove. The occurring variation refers to build-up-edges and wear of the rake face. The abrasive wear influences the measured width by relocating the cutting edge used as the origin during measurements. The steady state differs between VB_{max} = 150…200 µm because of the different distances of the groove on both of the tools used. After a tool life travel path of L_f = 2.686 m respectively L_f = 3.400 m the flank wear reaches the flank face behind the groove and leads to values above VB_{max} = 300 µm. The condition of the worn tools can be seen in Fig. 4. The scanning electron microscope (SEM) images were made by using a back scattered electron detector which represents the materials by different shades of grey. The cemented carbide is shown by light grey to near white, the workpiece material by medium grey and the material with a high portion of carbon as near black.

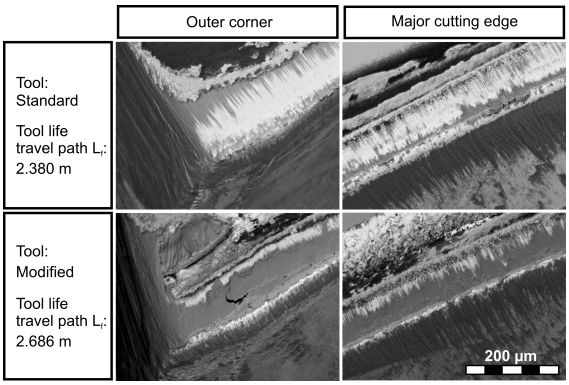

Fig. 4. SEM images of worn standard and modified twist drills

As can be seen both tools show extensive abrasive wear. The preparation of the cutting edge has been removed by the cutting process on both tools. The resulting edge has a radius below r = 10 µm. Abrasive wear occurs on the rake face and at the outer corner, too. Especially the modified tool shows a rounding of the outer corner which is additionally covered by adhesive workpiece material. The smeared material within the groove only occurs if wear reaches the flank face behind the modification. If the rounding of the corner gets too large or if too much of the remaining flank face before the groove has been abraded off, the rear edge of the groove gets in contact with the bore ground. This chipping leads to smeared material within the groove and it only occurs when the tool life has reached its end. The limitation of the flank wear by application of the groove can only be achieved at the outer corner. The image of the major cutting edge shows only about two thirds of the generated landing affected by abrasive wear.

A comparison of the amount of deposited workpiece material between the standard and the modified tool shows a much larger amount on the modified tool. The standard tool mostly shows Inconel 718 on the land and the rake face, while the modified tool has additional material on the flank face and the amount of workpiece material on the other faces is much larger. Furthermore the carbonaceous deposits reveal differ-

ences between both tools. These deposits consist of a large amount of carbon in combination with sulphur, phosphor and other elements and are attributed to boiling of the coolant. Because of the cleaning necessary for taking SEM images not all leftovers of the cutting fluid remain on the tools, as can be seen on the major cutting edge of the standard tool. The much larger amount of deposits on the standard tool indicates higher temperatures near the cutting edge. In comparison the modified tool only shows some small amounts of deposits in direct vicinity to the area of the flank wear.

4.2. Bore quality

The impact of the flank face modification on the bore quality is evaluated by the roundness deviation and the average surface roughness. The roundness deviation has been measured for the first 25 bores for each drill in different drilling depths. The parameters were chosen in accordance to VDI 2631 [33]. The average surface roughness was measured using a cut off filter of l_c = 0.25 mm in the first, fifth and tenth bore. Twelve measurement points were determined for each bore. The resulting boxplots are presented in Fig. 5.

The impact of the modified flank face on the variation of the roundness deviation is relatively small. Median and range of both tool types are identical. However the standard tool shows spikes above 0.020 mm. The influence on the average surface roughness is much more intense. As can be seen the maximum has been reduced from a value of about ΔRz =1 µm down to Rz = 5 µm. Both medians are close to each other, but the lower quantile of the modified tool reaches lower values and additionally the range of the values is smaller. Referring to both, roundness deviation and average surface roughness, the modification of the flank face does not influence the median of the measured values. Instead, the maximum has been reduced which is a hint for a more stable process. High values in roundness deviation result in most cases from small particles smeared onto the bore surface. High average surface roughness values are often influenced by marks caused by chips during evacuation. The decrease of high values can be used as an evidence that these undesired phenomena occur less when applying the modified drill.

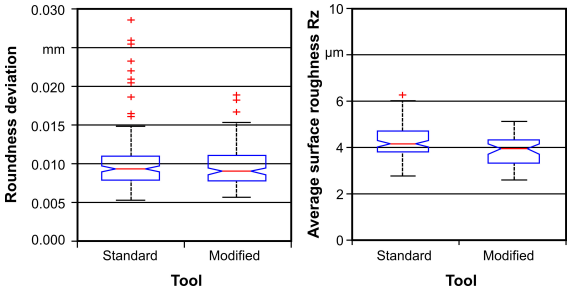

Fig. 5. Influence of the modified flank face on the bore roundness deviation and average surface roughness

4.3. Surface integrity of the bore

To investigate the surface integrity the first bore of each tool type were examined by light microscope images of the bore surface layer and by additional microhardness tests. Fig. 6 shows the results of the metallurgy preparation. After polishing Kallings 2 were used for etching. The figure represents the metallurgy of the bore surface layer within the axial direction. In radial direction no significant changes have been observed.

As it can be seen the microstructure of the basic material differs between the two samples. These differences are related to the position of the bores on the workpiece sample having a varying grain size across the diameter. Prior investigations showed only small impact of the grain size on the microhardness and a tendency to larger deformations of the grains within the bore surface layer according to larger grains. Fig. 6 reveals that both tool types alter the microstructure only to a depth of less than 20 µm. Changes in grain size and the tendency to a so called white layer limits to the first microns. Concerning to the higher deformation with increasing grain size the modified tool performs better. To summarize, the changes in microstructure for both tools are far below the typical limits given by the aerospace industry [34]. Further investigations were realized by microhardness tests which results are shown in Fig. 7. The horizontal lines mark the average hardness of the basic material.

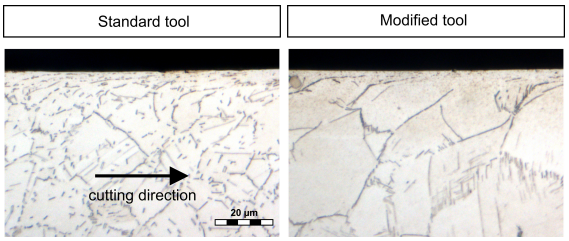

Fig. 6. Metallurgy preparation of the bore surface layer in axial direction

Both tools show higher hardness values up to a depth of 0.2 mm before the base hardness is reached. The standard tool reveals slightly larger values up to 100 HV0.025 in comparison to a maximum hardness of 75 HV0.025 when using the modified tool. The falloff with increasing distance to the bore is similar. The hardness tests are in compliance with the metallurgy inspections from Fig. 6. When using the modified tool the bore surface layer is slightly less influenced, but both tool types show good results.

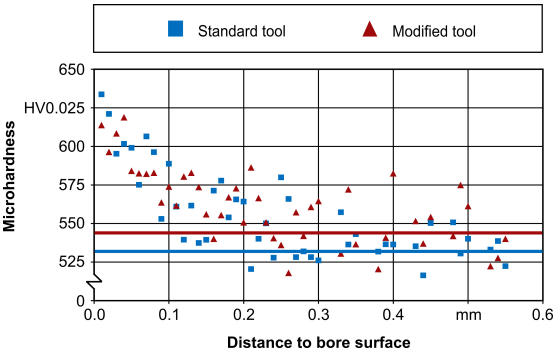

Fig. 7. Microhardness of the bore surface layer

5. CFD-Simulation results

Fig. 8 shows the velocity distribution of the fluid in the fringe zone of the bore ground and a sectional view of the flute. The sectional view for the *k*-ε model (Fig. 8) provides a

good insight to the core flow field but not near the boundary layers. The oscillatory contour-plots and a lower v_{max} are evidences that the velocity field is not accurately resolved. The *k-ω* model, however, cannot accurately resolve the core flow field but near the boundary layers. The advantage of this model is that the flow field near the boundary layers is resolved accurately, which is obvious with the plotted smooth contours in Fig. 8. The best results can be obtained by using the *k-ω*-SST model, which combines the advantages of both other models. The flow field can be resolved precisely in the complete domain by the *k-ω*-SST model.

Table 2 presents the comparison criteria for the examined turbulence models for the standard tool and the modified tool at two cross-sections along the cutting edge. The turbulence intensity shows that the *k-ω*-SST model resolves the temporal and spatial fluctuations in the boundary layers and in core flow areas much better than the other models. For all turbulence models, the modified tool results in a flow field which has a much higher maximum velocity, kinetic energy and volumetric flux inside the control area.

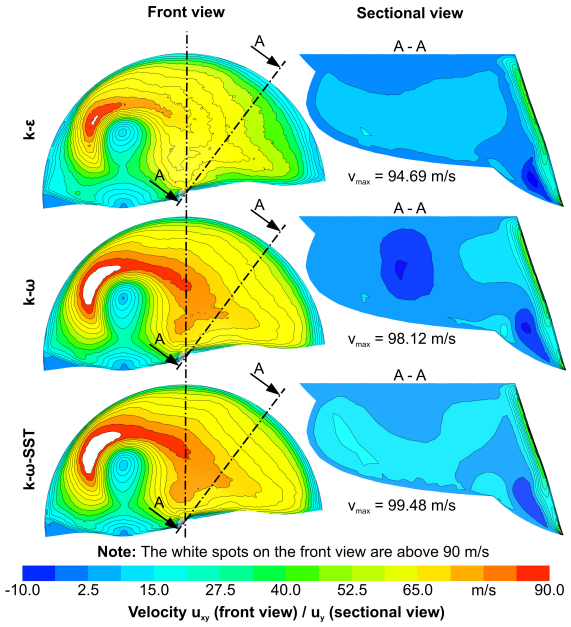

Fig. 8. Numerical results and comparison of the turbulence models in terms of the velocity

Table 2. Comparison of the turbulence models by numerical values

Turbulence model	*k-ε*	*k-ω*	*k-ω-SST*	Unit	
v_{max}	60.99	62.43	68.55	m/s	Standard tool
Re	7096.55	7264.57	7976.49	-	
k	15.28	16.21	19.09	m²/s	
I	0.0528	0.0526	0.0520	-	
Q	-	-	6.235E-03	m³/s	
v_{max}	71.93	77.55	87.15	m/s	Modified tool
Re	8370.15	9024.12	10141.35	-	
k	20.77	23.69	29.06	m²/s	
I	0.0517	0.0512	0.0501	-	
Q	-	-	1.036E-02	m³/s	

Fig. 9 shows that for the standard tool, the velocity values near the cutting edge decrease very quickly; and, at the outer corner the velocity is almost everywhere close to zero. The new flank face provides some space for the flow recirculation; so that, the momentum can be shifted more towards the edge. As a result, higher velocities of the coolant flow are achieved at the cutting edge and especially near the outer corner, see Fig. 9. This causes a higher amount of heat transport, hence a more effective cooling. A comparison of the coolant velocity distribution and the flank faces of the worn tools shows a good agreement regarding the relation between the low velocity regions and the deposits of burned coolant, especially around the outer corner.

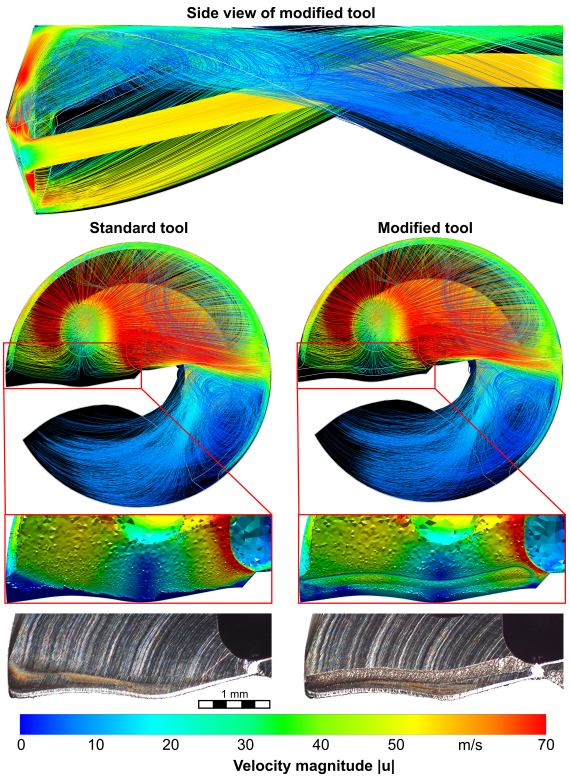

Fig. 9. Coolant velocity field and flank faces of the worn tools

6. Discussion

The use of a modified tool by modifying the flank face with a groove leads to different influences on the overall tool performance. Beside the improvement for tool life, the geometrical changes result in a better coolant supply for the thermally high loaded outer corner where the maximum wear occurs. The tool life is increased due to the fact that the width of the flank wear land is limited and a wear stock is achieved by the groove. The improved coolant flow occurs due to the larger hydraulic diameter close to the cutting edge and due to a channeling effect through the groove. The CFD simulations show that the modified tool provided a better coolant flow. An evidence for good agreement of our experimental and numerical studies is the accordance of the deposits of coolant on the tool and the resulting flow field on the flank faces, see Fig. 9.

A lower amount of deposits indicate lower temperatures within the cutting zone. By reducing the hardness loss of the cemented carbide the latter support a longer tool life time. Therefore, the tool life increases up to 50%, as shown in section 4.1. Beside the increase in tool life, the modified tool shows a better performance regarding to the bore quality. The absence of high values for roundness deviation and average surface roughness can be related to the better lubrication. Better cooling and lubrication also improves the surface integrity as shown in Fig. 6 and 7.

7. Conclusion

The presented results show that the modification of the flank face can improve the overall performance of cemented carbide drills while machining Inconel 718. The designed groove extends the tool life up to 50 % and additionally leads to a much better coolant supply to the high loaded parts of the drill. To analyze the coolant flow a three-dimensional, steady CFD-simulation has been used. The very small geometrical features near the cutting edge lead to a challenging meshing process and a high number of nodes. The comparison of the turbulence models showed that only the k-ω-SST is suitable to numerically simulate the coolant flow in the complete domain. With the experimental results, the impact of the modified flank face can be analyzed in detail. The numerical and experimental results are found to be in agreement.

The results are very encouraging for the development of additional improved tools with geometrical modifications. Within further investigations more complex flank faces can be designed and studied. The CFD-simulation provides a good support at the design stage by reducing the number of prototypes to be tested in upcoming experimental work. Additionally, it allows the detailed analysis of the coolant flow, which cannot be measured with the state-of-art techniques.

Acknowledgements

The authors would like to thank the Guehring KG, Albstadt, Germany, for supporting this research.

References

[1] Donachie MJ, Donachie SJ. Superalloys. Ohio: ASM; 2008
[2] Zhang L, Wagner T, Biermann D. Optimization of cutting parameters for drilling Nickel-based alloys using statistical experimental design techniques. In: Hinduja S., Li L. Proceedings of the 37th International MATADOR Conference. London: Springer; 2013. p. 123-126.
[3] Ezugwu E. Key improvements in the machining of difficult-to-cut aerospace superalloys. Int J Mach Tool Manu 2005;12-13:1353-67.
[4] Sharman A, Amarasinghe A, Ridgway K. Tool life and surface integrity aspects when drilling and hole making in Inconel 718. J Mater Process Technol 2008;1-3:424-32.
[5] Ezugwu E, Wang Z, Machado A. The machinability of nickel-based alloys: a review. J Mater Process Technol 1999; 1-3:1-16
[6] Chen Y, Liao Y. Study on wear mechanisms in drilling of Inconel 718 superalloy. J Mater Process Technol 2003; 1-3:269-73.
[7] Veselovac D. Process and product monitoring in the drilling of critical aero engine components. Aachen: Apprimus Verlag; 2013
[8] Rahim EA, Sasahara H. An Analysis of surface integrity when drilling inconel 718 using palm oil and synthetic ester under MQL condition. Mach Sci Technol 2011; 1:76-90.
[9] Aurich JC, Fallenstein F. CFD-Simulation der Kühlung von innengekühlten VHM-Wendelbohrern. VDI-Z Special Werkzeuge 2013; II:48-51.
[10] Gühring OHG: Kühlkanal-Geometrie 2003; DE20321908U1.
[11] Hänle P, Schwenck M. Optimization of Cutting Tools using CA-Technologies. In: Neugebauer R. Proceedings of the 8th CIRP International Workshop on Modeling of Machining Operations. Chemnitz: Verlag Wissenschaftliche Scripten; 2005. p. 463-68.
[12] Obikawa T, Yamaguchi M. Computational Fluid Dynamic Analysis of Coolant Flow in Turning. Procedia CIRP 2013; 8:271–75.
[13] Vollmer R, Stihler H. Wendeschneidplatte 1993; DE4319505C2.
[14] Bergmann B. Studie zu Freiflächengeometrien beim Hartfräsen liefert erste Ergebnisse. VDW Branchenreport 2012; 12:15-16.
[15] Meyer R. Neue Schneidengeometrien zur Verbesserung des Werkzeugeinsatzverhaltens beim Hartdrehen. Garbsen: Produktionstechn. Zentrum; 2011.
[16] Denkena B, Ben Amor R. Hartbearbeitungswerkzeug für die spanende Bearbeitung gehärteter Werkzeuge 2006; DE102006020613B4.
[17] Opalla D. Hochleistungsbohren metallischer Werkstoffe mit Wendelbohrern. Essen: Vulkan Verlag; 2003.
[18] Terwey I. Steigerung der Leistungsfähigkeit von Vollhartmetall-wendelbohrern durch Strahlspanen. Essen: Vulkan Verlag; 2011.
[19] Wessels T. Bohren in Titan- und Nickelbasislegierungen. Essen: Vulkan Verlag; 2007.
[20] Biermann D, Beer N, Sattel S. Führungsfaseneinfluss beim Bohren – Nickelbasislegierung Inconel 718 mit hoher Oberflächengüte bearbeiten. VDI-Z Special Werkzeuge 2013; I:28-30
[21] Biermann D., Beer N, Zhang L. Bohrbearbeitung der Superlegierung Inconel 718 – Einfluss von Bohrergestalt und Beschichtung auf das Bearbeitungsergebnis. wt online 2013; 7/8:437-42.
[22] Norton T, Sun DW, Grant J, Fallon R, Dodd V. Applications of computational fluid dynamics (CFD) in the modelling and design of ventilation systems in the agricultural industry: A review. Bioresour Technol 2007; 12:2386-414.
[23] Versteeg HK, Malalasekera W. An introduction to computational fluid dynamics. Harlow: Pearson Education Ltd; 2007.
[24] Özkaya E, Bayraktar E, Turek S, Biermann D. A novel abrasive blasting process: Abrasive medium classification and CFD simulations 2013; 44:6, p. 577-88.
[25] Özkaya E, Bayraktar E, Turek S, Biermann D. Abrasive medium classification and CFD simulations for low-pressure abrasive water-jet blasting. Ergebnisberichte des Instituts für Angewandte Mathematik, Technische Universität Dortmund 2013; p. 469.
[26] Biermann D, Özkaya E. Abrasivstrahlsystem für schwer zerspanbare Bauteile. Mikroproduktion 2013; 1:38-41.
[27] Bayraktar E, Özkaya E, Münster R, Biermann D, Turek S. Nozzle Design for Low-Pressure Micro Abrasive Waterjet Blasting via CFD Simulations. Ergebnisberichte des Instituts für Angewandte Mathematik, Technische Universität Dortmund 2013; p. 465.
[28] Sahili A, Zogheib B, Barron RM. 3-D Modeling of Axial Fans. Ima J Appl Math 2014; 4:632-51
[29] Brochu T, Batty C, Bridson R. Matching fluid simulation elements to surface geometry and topology. ACM Transactions on Graphics 2010; 4:1-9.
[30] Holloway MV, Beasley DE, Conner ME. Investigation of Swirling Flow in Rod Bundle Subchannels Using Computational Fluid Dynamics. 14th Proceedings of ICONE14. Miami, 2006. p. 1-11.
[31] Rahimi M, Parvareh A.: Experimental and CFD investigation on mixing by a jet in a semi-industrial stirred tank. Chem Eng J 2005; 1-2:85-92.
[32] Kalitzin G, Medic G, Iaccarino G, Durbin P. Near-wall behavior of RANS turbulence models and implications for wall functions. J Comput Phys 2005; 1:265-91.
[33] VDI2631-3: Formprüfung - Eigenschaften und Auswahl von Filtern. Berlin: Beuth; 2007.
[34] Glaser JD. Einlippenbohren von hochwarmfesten, schwer zerspanbaren Nickelbasierungen. Essen: Vulkan Verlag; 2010.